A Novel Method For Removing Baseline Drifts in Multivariate Chemical Sensor

Abhishek Grover, Brejesh Lall

***Abstract*—This paper proposes a sensor signal processing method for removing baseline drifts in multimodal chemical sensors. Sensitivity and baseline drift are the primary reasons for inaccurate readings from low-cost sensors. The prediction errors from state of the art multivariate regression algorithms have been high due to the drifts. The response of a sensor is modeled as an Auto-Regressive (AR) process associated with an observation zero-mean Gaussian noise. The parameters of the state space model are learned using calibration data. The variance of the Gaussian noise is estimated using an adaptive online method. The AR process equation and observation equation are used to construct the adaptive Kalman filter. Each sensor response is passed through a separate Kalman filter, and then a regression technique is used to predict the sensor response. The proposed model is applied on a standard air quality dataset to demonstrate its efficacy in removing drifts in sensors.**

***Index Terms*—Air Pollution, Sensor Array, Kalman Filter, Drift Correction, Calibration, Chemometrics**

I. Introduction

Low-cost Multivariate sensors such as Metal Oxide (MOX) sensor arrays have been extensively used for gas quantification and classification applications [1]. Their major advantage is a small form factor, low-cost, and wide availability of MOS fabrication facilities. Low-cost sensors have been proven useful for air pollution measurement applications as they help in capturing pollutant information at high spatial density [2]. Chemical sensors have been used for gas leakage detection [3] and localization applications [4]. Low-cost sensors find applications in pollutants detection in industrial environment [5], and other e-nose applications [6]. The primary concern with low-cost sensors is their low-reliability [7][8]. The response of such sensors has been found to vary with changing meteorological conditions [9]. The aging effect is also pronounced in such sensors [10]. Cross-sensitivity in gas sensors is another reason for inaccurate readings [11]. Low-cost sensors have been associated with two kinds of drifts. One is the sensitivity drift or device drift, and the other is the baseline drift [12]. The device drift occurs due to the aging or poisoning effect in the sensor due to continuous deposition of contaminants on sensor film over time. It is usually due to chemical diffusion of oxygen vacanices and physical changes in film over time [13]. The baseline drift is due to variation in ambient environmental conditions. The resistance change in sensors is highly sensitive to temperature and humidity variations. The combination of these two effects make low-cost chemical sensors unreliable for independent measurement applications. A MOX chemical sensor system consists of an array of MOX sensors in which each sensor has a specific sensitivity towards a pollutant. In presence of a chemical, each sensor responds uniquely based on the selectivity of specific sensor film material. Usually pattern recognition techniques are used to estimate the actual measurend value based on responses from sensors [14]. Various kinds of data analytics tools have been used for robust and accurate calibration [15]. Typically, the multivariate nature of the sensor readings has been used to calibrate the sensor units. The calibration process can be understood as a combination of feature extraction and regression model. The feature extraction is used to extract the features of the multivariate signal obtained from the sensor unit. The regression model is built using a training set with the features as the independent variables and the actual measurend values as the dependent variable. The major problem in e-nose sensing lies in the regression model used for calibration. Many studies have shown the utility of Artificial Neural Networks [16][17], Support Vector Regression [18] and Partial least square [19]. These techniques perform very well on the training set or calibration set but provide erroneous results on same sensors deployed in the field. The reason for this underperformance is the shift in data statistics of the sensor signal when it is deployed in the field. This shift occurs due to sensitivity and baseline drift. Thus a suitable baseline drift removal technique would help in increasing the accuracy and robustness of the regression algorithms.

This paper proposes a signal processing technique for removing baseline drifts in a chemical sensor array. A bank of Kalman filter has been used to remove drift effects in the sensor array. The calibration data of the sensor is used to learn the system dynamics of the sensor. The system dynamics are represented in the form of a state space model. The other part of the signal model is the observation equation. The observation equation is associated with an observation noise which quantizes the deviation of observations from the learned system dynamics. The observation noise is calculated using an adaptive technique. Each sensor signal is passed through a particular Kalman filter, which predicts an optimal estimate of the sensor signal based on the dynamics and noise variance. The filtered signal samples is then used as independent variable in multivariate regression to predict the sensor response. The proposed model has been applied to an air quality dataset [20]. The proposed approach increases the robustness of regression models to drifts in sensors. It results in lower mean absolute errors from regression models. It presents a set of parameters that can be used for factory calibration of sensors. The additional advantage is that the proposed

The authors are with Bharti School of Telecommunication Technology and Management, Indian Institute of Technology Delhi, Hauz Khas, New Delhi-110016. Email id: abhishekgrover13@gmail.com, brejesh@ee.iitd.ac.in.

approach can be applied in other chemometric applications as well.

The contributions of this paper are as follows:

- A novel method for removal of baseline drifts has been presented.
- The method is based on modeling the system dynamics as a state space model. The parameters of the model have been learned using calibration data.
- The proposed approach enables easy calibration in factory setting.
- The method has been tested on a standard dataset for CO, C_6H_6, NO_x and NO_2 concentration levels.

The organization of this paper is as follows. Section 1 is an Introduction, Section 2 is Related Work and Section 3 is Sensor Calibration, Section 4 is Results and Discussion, and Section 5 is Conclusion and Future Scope.

II. Related Work

Chemical sensor array data is essentially a multivariate time series. It is to be noted that in this discussion, sensor array implies a sensor with multivariate response. The signal processing techniques for drift compensation can be characterized into univariate and multivariate techniques [21]. In univariate methods, preprocessing for drift correction is applied to each sensor independently. A classical univariate method is the baseline removal method used in spectroscopic analysis [22]. It involves transforming the signal to frequency domain using Fast Fourier Transform (FFT), removing the undesired frequency components and then using the inverse FFT to reconstruct the baseline removed signal. Methods using time series analysis and Discrete Wavelet Transform (DWT) can also be classified as univariate methods. Time series data always have latent information related to the evolution of samples. There have been efforts for modeling the sensor response using time series analysis [23][24], but most of the recent efforts are entirely based on machine learning methods. Time series features have been used for developing kernels in support vector regression for machine olfaction application [25]. A notable effort for drift compensation using extended Kalman filter has been implemented for Surface Acoustic Wave (SAW) sensors [12]. A similar attempt using SAW sensors has been implemented for the detection of aromatic compounds in water [26]. There were some drawbacks for these implementations. It requires the sensor response to be quantified in form of a mathematical equation to express the state space model, which is not possible to develop for many chemical sensors such as MOX sensors. It requires the gas concentration to be repeatedly applied and flushed away from the sensor so that the baseline stabilises after each measurement. Such an arrangement cannot be achieved for open sampling systems which is the use case in this study. In wavelet analysis [27], the signal is decomposed using DWT into signal coefficients which represent the low and high frequency bands. The coefficients with values less than a threshold are nullified and then the signal is reconstructed using inverse DWT. The obtained signal is essentially drift free since the drift predominantly lies in the low frequency spectrum. Short time Fourier transform has been used for incresing robustness of odor classification [28].

In multivariate techniques, compensation is applied across the sensors. Techniques such as Orthogonal Signal Correction (OSC) and calibration transfer can be classified in this category. In OSC [29][30], the principal components of the data matrix containing sensor responses which account for maximum variance and are orthogonal to measurend response vector are identified and removed from the data matrix. The basic idea for this method is that drift is associated with principal components that are orthogonal to the response vector. The major disadvantage of this method is its over-reliance on calibration data. Dynamic principal component analysis has been used for the application of leakage detection [31]. This method was based on selecting drift independent features as input for regression. Several machine learning approaches have been proposed for drift compensation in e-nose applications. Extreme learning machines have been used in classification applications [32]. A cross-domain subspace algorithm has been suggested [6] as a solution. A transfer learning approach with autoencoders has also been implemented [33]. The practical feasibility of these solutions is limited due to two reasons. Firstly, the methods rely completely on calibration data learned during the initial phase of sensor life. The operating characteristics of sensors changes drastically during its lifetime. Secondly, developing a calibration model for a specific device is also a challenge since the operating characteristics of a chemical sensor varies from device to device.

The proposed model removes the demerits of the above implementations and gives a new direction for experimental calibration based on data-driven system identification techniques and online parameter estimation for the sensor model.

III. Sensor Calibration

Most machine learning-based techniques in the area of sensor calibration have focussed on learning the data statistics, which is not a good choice because of the baseline shifts and inter-dependence of temporal samples. Instead of learning the data statistics, the calibration model should learn the system dynamics. For a given dataset, one can surely obtain a low mean absolute error by tuning the model parameters of ML techniques, but it is difficult to say whether the model is a suitable generalization of underlying data generation mechanism or not. Machine learning models should be carefully used for time series application since the chances of overfitting of data are very high. The proposed calibration scheme utilizes the combination of time series analysis and ML techniques. Time series analysis has been used to model the sensor signal and multivariate regression techniques for concentration prediction.

The system dynamics can be learned in two ways: one is by modeling the operation of a sensor using the physical laws, and the other is the data-driven modeling. Regression techniques [14] have always been used for gas sensing applications because it is complicated to quantize the operation of the gas sensor array using physical laws. Therefore we too would be using the data-driven approach for learning the system

This article has been accepted for publication in a future issue of this journal, but has not been fully edited. Content may change prior to final publication. Citation information: DOI 10.1109/TIM.2020.2976224, IEEE Transactions on Instrumentation and Measurement

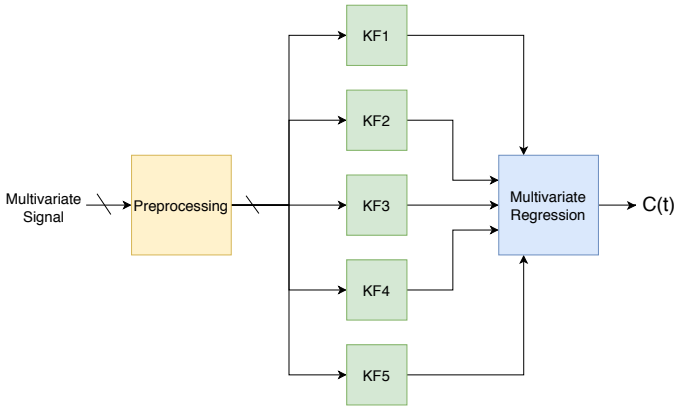

Fig. 1: Calibration model; KF1, KF2, KF3, KF4 and KF5 are Kalman filters for each sensor signal. C(t) is the predicted concentration at time instant t.

dynamics. System identification [34] deals with developing a grey-box or black box model of an underlying system. The process consists of first identifying a structure, then finding its parameters, and the last step is validation of the obtained model. Figure 1 depicts the calibration model proposed in this study. The model consists of a preprocessing stage, followed by Kalman filter bank to filter the sensor signal (to account for drifts in sensor response) and a multivariate regression technique to predict concentration level. The present study is based on sensor data of 5 sensors in an array. It is due to this reason that figure 1 shows 5 filters. For each sensor, a specific filter has been used to account for drift in the response. Subsection 2.1 explains the preprocessing required on sensor response signal. Subsection 2.2 and 2.3 explain the procedure for estimating the parameters of the proposed Kalman filter. The analysis in these subsections is for a scalar signal which is the output of one sensor in the MOX sensor array package. The similar analysis is repeated for all sensors in the sensor package and is used in constructing the Kalman filter for the specific sensor response. Thus the Kalman filter bank shown in figure 1 consists of filters with parameters specific to the particular sensor in sensor array. Subsection 2.4 mentions the regression techniques used in this study.

A. Preprocessing

The first stage is the preprocessing stage. This stage consists of log transformation of data followed by first-order differencing as shown in equation (1),

$$x_t = z_t - z_{t-1} \tag{1}$$

where z_t is the log of sensor response value at a specific instant and x_t is the differenced output. The log transformation has been used for two reasons. Air quality data is usually positively skewed, which leads to a positively skewed sensor response. The transformation helps in reducing the skewness level. The other reason is to minimize the variance spread of the signal. The reason for differencing operation is to stabilize mean of the signal. These two operations have been implemented so that the signal properties can be assumed similar to that of a stationary signal. The physical interpretation for advantages of differencing operation can be understood as follows. The consecutive samples of the sensor signal are affected by similar sensitivity drift and interference effects. Hence differencing operation removes the drifts and baseline effects, and the outputs of signal processing operations that we apply on the differenced signal are essentially free of baseline drift effects.

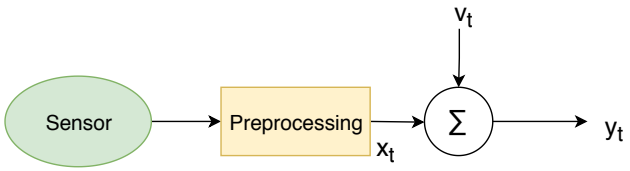

$$x_t = \phi x_{t-1} + w_t \qquad w_t \sim N(0, Q)$$
$$y_t = x_t + v_t \qquad v_t \sim N(0, R)$$

Fig. 2: Sensor Signal model

B. System Identification

The signal model has been depicted in figure 2. The system is modeled using state space equation given in (2) and (3). Equation 2 is the state transition equation and equation 3 is the observation equation.

$$x_t = \phi x_{t-1} + w_t \qquad w_t \sim N(0, Q) \tag{2}$$

$$y_t = x_t + v_t \qquad v_t \sim N(0, R) \tag{3}$$

The output x_t, preprocessed signal, has been modeled as an autoregressive process of order one. The transition scalar of AR process is ϕ. The variance of the associated process noise is Q. This process is associated with an observation noise v_t, which represents variation in sensor response due to sensor aging or change in environmental conditions between calibration and testing time. The variance for observation noise is denoted as R. The individual Kalman filters, shown in figure 1, are used to estimate the correct underlying state x_t using observation y_t, noise parameters Q and R, and AR parameter ϕ. The underlying philosophy for this pre-filtering before regression is as follows. Calibration data is an essential part of chemical sensing applications. The significant prediction errors that arise in such applications is due to the shift in environmental conditions and sensor poisoning/aging effects. These variations make the calibration model obtained using training data ineffective as with same ambient pollutant levels sensors are giving values corrupted with drifts. By using a state transition equation, we have ensured that sensor readings will always evolve as per the time series model learned during calibration time. The Kalman filter assimilates the information from the model and observations and provides an optimal estimate of the underlying signal [35]. The regression technique predicts the pollutant concentration using the optimal estimate predicted by the Kalman filter. The parameters ϕ and Q are obtained using training data.The maximum likelihood procedure [36] is used to obtain parameter values. These methods are sensitive to initial estimates. In this study, the initial estimates

are obtained using the autocorrelation and covariance function of the observed time series. Using equation 2 in a recursive manner and stationarity assumptions we can derive equation 4.

$$x_t = \phi^k x_{t-k} + \phi^{k-1} x_{t-k-1} + ... + w_t \tag{4}$$

Multiplying x_{k} both sides of equation 4 and taking expectation both sides leads to equation 5, where $\gamma(k)$ is the covariance of sample values at time instant t and $t-k$.

$$\gamma(k) = \phi^k E[x_{t-k} x_{t-k}] = \phi^k \gamma(0) \tag{5}$$

Multiplying by $x_{\mathrm{t\text{-}1}}$ both sides of equation 2 and taking expectation leads to eqaution 6.

$$\gamma(0) = \phi\gamma(1) + Q \tag{6}$$

Equation 7 can be derived by using equation 5 and 6. Here γ_x and γ_y specifically denotes the covariance of underlying state and observations. The two can be related using equation 8.

$$\gamma_x(k) = \frac{Q}{1-\phi^2}\phi^k \tag{7}$$

$$\gamma_y(k) = Cov(y_t, y_{t-k}) = Cov(x_t + v_t, x_{t-k} + v_{t-k}) \tag{8}$$

Equation 8 shows that $\gamma_y(k) = \gamma_x(k)$, under the assumption that noise and state values at different instants are independent. This shows that the covariance of underlying state is similar to observations. The autocorrelation function for observations y can be obtained using equation 9.

$$\rho_y(k) = \frac{\gamma_y(k)}{\gamma_y(0)} = \frac{\gamma_x(k)}{\gamma_y(0)} \tag{9}$$

$$\frac{\hat{\rho_y}(2)}{\hat{\rho_y}(1)} = \phi^0 \tag{10}$$

$$Q^0 = \frac{(1-{\phi^0}^2)\hat{\gamma_y}(1)}{\phi^0} \tag{11}$$

Equation 10 is obtained using equation 9 and 7 where ϕ^0 is the initial estimate for ϕ. The initial estimate for $Q(Q^0)$,shown in equation 11, is obtained using equation 10 and 7. These initial values are then used in maximum lilelihood algorithm for parameter estimation.

C. Online Parameter Estimation

The static parameters ϕ and Q are determined using training data. The observation noise variance R is calculated using an online technique. Assume x_t^f to be the forecast value obtained using the state transition equation. The Kalman filter assimilates this forecast information from the transition model and the new observation to find an estimate of the underlying state. Let y_{t} be the observation which is associated with an additive zero mean Gaussian noise of variance R. The following equations represent the standard form for Kalman filter measurement update equations [35].

$$\hat{x}_t = x_t^f + K_t(y_t - x_t^f) \tag{12}$$

$$K_t = \frac{P_t^f}{P_t^f + R} \qquad where \quad P_t^f = E[(x_t - x_t^f)^2] \tag{13}$$

$$\hat{P}_t = E[(x_t - \hat{x}_t)^2] = (1-K_t)P_t^f \tag{14}$$

The innovation sequence ε_t and its variance can be expressed using equations 15 and 16.

$$\varepsilon_t = y_t - x_t^f \tag{15}$$

$$E[\varepsilon_t^2] = E[((x_t - x_t^f) + v_t)^2] = P_t^f + R \tag{16}$$

Equation 16 expresses R as the difference of the innovation variance and the forecast error variance. Updating R using equation 16 is known as innovation based adaptive estimation. The specific method is known as covariance matching and has been used for chemical sensing [37] and Inertial Navigation System (INS) applications [38]. The major problem with this method is that it does not ensure a positive value of R. The residual sequence can also be used to update the value of R The residual sequence η_t and its variance can be expressed using equations 17 and 18.

$$\eta_t = y_t - \hat{x}_t \qquad and \quad \eta_t = (1-K_t)\varepsilon_t \tag{17}$$

$$E[\eta_t^2] = (1-K_t)^2 E[\varepsilon_t^2] \tag{18}$$

Equation 20 can be derived using equation 18 and 13.

$$E[\eta_t^2] = \frac{R}{P_t^f + R}(1-K_t)(P_t^f + R) = R - RK_t \tag{19}$$

$$R = E[\eta_t^2] + \hat{P}_t \tag{20}$$

Equation 20 demonstrates that R can be calculated as the sum of the variance of the residuals and the variance of the estimation error. This equation helps in estimating R in an online routine. This method is known as residual based adaptive estimation [38][39]. The following equations 21 and 22 are used for adaptive estimation of R, where $\hat{R}_k$ is the estimate of observation noise variance. The subscript k denotes the index of the block of N samples for which a specific R_{k} is used. The value of R is updated using its prevoius value and the newly obtained estimate as given in equation 22.

$$\hat{R}_k = \frac{1}{N}\sum_{i=1}^{N} E[\eta_t^2] + \frac{1}{N}\sum_{i=1}^{N} \hat{P}_t \tag{21}$$

$$R_k = (1-\alpha)R_{k-1} + \alpha\hat{R}_k \tag{22}$$

After every N observations, the residuals are used to calculate the variance which is used in Kalman filter algorithm for next N observations.

The value α, in equation 22, controls the weight given to the new estimate of R. It controls the rate of change of variance of observation noise with time. The value of α depends on the sensor material and pollutant to be measured. It should be selected based on experimental analysis similar to the one proposed in this study.

It should be noted that the method is easily scalable for large sensor arrays. The computations presented above can be converted into matrix computations by assuming the sensor responses as a vector of observations. Thus the univariate state space models presented above can be depicted in form of a multivariate state space model and equations can be derived in a similar manner using matrix algebra. The noise matrices and

transition matrix in the multivariate case can be assumed to be diagonal since the response of each sensor is independent of other sensors. Thus the comutational complexity of the algorithm is minimal in view of the matrix computations capability available in low cost microcontrollers.

D. Multivariate Regression

The filter output is essentially the optimal estimate $(\hat{x_t})$ of differenced signal (x_t; as shown in equation 1). This is converted into absolute value by adding previous time instant value z_{t-1} to $\hat{x_t}$. The obtained absolute values of each sensor in an array is given as input to the multivariate regression block shown in figure 1. The regression model is learned using a calibration dataset. We have evaluated our model using three techniques: Support Vector Regression (SVR), Partial Least Square (PLS) Regression, and Multivariate Linear Regression (MVLR). Previous studies [14][40] have shown that low absolute mean errors can be obtained using advanced machine learning techniques such as neural network and support vector regression, but one should always be careful while applying such techniques in chemical sensing applications which have a limited calibration dataset. We can achieve low errors for a given dataset by tuning parameters, but it is highly unlikely that we might get similar results for another dataset. Tuning the parameters to account for every data point in training set might lead to overfitting of data and low generalisability of the model. For example, in support vector algorithm, if the number of support vector is close to the number of data points in the training set, then that means the algorithm has just learned the data points and is unable to learn the data generation pattern. Such an algorithm might work on the training set or for very similar datasets, but it might not work for arbitrary dataset. In addition to this, variation in environmental conditions may lead to a shift in statistics of pollutant concentration, thus making the algorithm ineffective. A simpler algorithm might prove more useful for chemical sensing data. This is evidenced by the various implementations in chemical sensing literature [14]. PLS has been considered to be the gold standard for chemical sensing [14]. In PLS, first, the principal components which capture the maximum covariance between predictors and dependents are identified, and then ordinary least square regression is used for concentration prediction. The SVR algorithm was designed using the parameters $\epsilon = 0.2$, $\gamma = 16$ and $C = 512$. In SVR, ϵ is the distance of maginal hyperplane from the regression hyperplane, γ is the Gaussian kernel parameter and C is the constant that penalizes the points lying outside the marginal hyperplanes [41]. The predictions in PLS were calculated based on the 3 principle components which captured the maximum covariance in training set. The mean absolute error (MAE), root mean square error (RMSE), and Coefficient of Determination (R^2) have been used to compare the results obtained in this study.

IV. Results and Discussion

A. Data and Statistical Tools

The dataset consists of vector time series (with 5 elements) sampled once every hour. The sensor array consisted of 5 chemoresistive sensors. Each sensor has selectivity for specific pollutant. Each sensor response corresponds to readings from one of the 5 sensors in the array. The dataset also contains the actual pollutant concentration levels of carbon monoxide (CO) in mg/m^3, benzene (C_6H_6) in μg/m^3, oxides of nitrogen (NOx) in ppb, and nitrogen dioxide (NO_2) in μg/m^3. The length of the dataset available [20] is 7100 Hrs. There is always a trade off in selection of training set lengths for such applications. A small length might lead to large test errors while a large length might lead to low test errors but the learned model in this case is based on data statistics corrupted by drifts. A large training time also increases the factory calibration duration. An optimal length for a specific application can be identified based on experimental study. To ensure that the training time is not exorbitantly long, we have chosen 500 hrs as the length of training set. The remaining dataset was used as the test set. A subset of numerical results has been presented for the case of training lengths as 300 hrs and 700 hrs. This has been implemented to demonstrate the trade off in selection of training set length. The low-cost sensor responses are in terms of resistivity of sensors. The range of concentration values for the period of measurement are: CO (0.1-11.9 mg/m^3), C_6H_6 (0.2-63.7 μg/m^3), NOx (2-1479 ppb) and NO_2(2-288 μg/m^3).

The parameters proposed in section 2.2 have been calculated using the maximum likelihood procedure available in package MARSS [42] in R. The Kalman filter was constructed using the functions available in package dlm [43]. The support vector regression algorithm has been implemented using package e1071 [44]. The pls [45] package has been used to implement partial least square regression.

	Model	Training MAE	Test MAE	R^2	RMSE
CO					
	M1	0.23	1.12	0.01	1.46
	M2	0.40	0.85	0.30	1.23
	M3	0.40	0.96	0.18	1.33
C_6H_6					
	M1	1.26	5.65	0.02	7.53
	M2	1.52	2.76	0.72	3.98
	M3	1.47	3.13	0.66	4.46
NOx					
	M1	13.96	140.90	-0.17	222.40
	M2	26.47	135.30	-0.11	215.74
	M3	26.59	139.60	-0.15	220.30
NO_2					
	M1	5.37	31.46	0.01	40.23
	M2	11.14	22.59	0.41	30.97
	M3	11.08	22.07	0.44	30.18

TABLE I: Error parameters using only pattern recognition techniques; M1: SVR, M2: PLS, M3: MVLR

B. Numerical Results

Table I depicts the results for the application of only multivariate regression techniques on sensor array response. The important conclusions from table 1 are as follows: For each pollutant, the simpler techniques PLS and MVLR perform better than SVR. The results for PLS are the best. The R^2 parameter for MVLR and PLS is much better than SVR which shows that the simpler models are more effective in capturing the variability in data. Lower RMSE in PLS also

	$\alpha = 0.001$					$\alpha = 0.002$				$\alpha = 0.003$			
	Model	Training MAE	Test MAE	R^2	RMSE	Training MAE	Test MAE	R^2	RMSE	Training MAE	Test MAE	R^2	RMSE
CO													
	M1	0.23	1.13	0.01	1.46	0.23	1.12	0.01	1.46	0.23	1.12	0.02	1.46
	M2	0.40	0.87	0.39	1.20	0.40	0.92	0.33	1.20	0.40	1.01	0.26	1.27
	M3	0.40	0.81	0.42	1.11	0.40	0.86	0.42	1.11	0.40	0.97	0.34	1.20
C_6H_6													
	M1	1.26	5.63	0.02	7.51	1.26	5.61	0.02	7.50	1.26	5.60	0.03	7.48
	M2	1.52	3.17	0.64	4.54	1.52	3.42	0.62	4.70	1.52	3.97	0.53	5.22
	M3	1.47	2.26	0.83	3.17	1.47	2.61	0.80	3.42	1.47	3.31	0.70	4.17
NOx													
	M1	13.96	140.79	-0.17	222.24	13.96	140.65	-0.17	222.08	13.96	140.55	-0.17	221.92
	M2	26.47	127.40	0.01	203.81	26.47	120.05	0.11	194.02	26.47	116.12	0.16	187.76
	M3	26.59	126.42	0.02	202.95	26.59	118.79	0.12	192.59	26.59	114.66	0.18	186.13
NO_2													
	M1	5.37	31.40	0.01	40.17	5.37	31.36	0.02	40.11	5.37	31.30	0.02	40.04
	M2	11.14	24.83	0.35	32.68	11.14	24.50	0.37	32.03	11.14	24.36	0.39	31.63
	M3	11.08	21.95	0.46	29.72	11.08	21.92	0.47	29.40	11.08	21.98	0.48	29.20

TABLE II: Error parameters using proposed calibration model for $\alpha = 0.001$, $\alpha = 0.002$, and $\alpha = 0.003$; Three pattern recognition techniques (M1: SVR, M2: PLS, M3: MVLR) were used for analysis.

shows that outliers are much better handled using simpler techniques.The variation in MAE from model to model is large for all pollutants. The support vector count in case of SVR is close to 350 out of the total 500 data points used in the training set. The training MAE of SVR is best for all cases, but the test MAE is worst. This shows that the complex routines primarily learn the training data points, and their performance degrades drastically when the data statistics shift. Table I essentially proves the robustness of simpler learning algorithms and their utility in modeling responses of air pollutant concentrations from low-cost sensors. The application of the Kalman filter proposed in this study is to complement this robustness with a sensor drift correction method. Figure 3 shows the sensor response with and without the application of the adaptive Kalman filter. The filtered sensor responses (black) follow the original sensor responses (blue) for the initial part of the time series, and it starts to drift for the latter part of the time series. This drift is due to the variation of sensor response in comparison to that learned during calibration time. This variation is captured in terms of the noise variance of the observation equation. The noise variance of the observation equation is changed as time passes by, based on the residuals of the Kalman filter. The amount of drift can be controlled by the parameter α. The parameter α should be selected based on experimental analysis. Figure 3 helps in understanding the role played by the adaptive Kalman filter proposed in this application. The filter constantly monitors the observations and adjusts its observation variance based on the obtained residuals. This ensures that the time series of sensor responses evolves in accordance with the state transition equation learned during calibration.

Table II represents the result of the proposed calibration model. The value of N used in this study is 50. Three values of α (0.001, 0.002, 0.003) were chosen based on low MAE criteria. The errors were lowest for $\alpha = 0.001$ in case of CO and C_6H_6. For NOx and NO_2, the value of $\alpha = 0.003$ was the best. The value $\alpha = 0.002$ gives average low error for all pollutants. This brings out a peculiar characteristic of low-cost sensor responses. The amount of sensor drift is highly variable for each sensor and depends on sensor material and the pollutant to be measured. Table II shows that MVLR gives the lowest MAE and RMSE errors and the highest R^2. This

	Phase	CM1	CM2
CO			
	1	0.73	0.84
	2	1.18	0.90
C_6H_6			
	1	1.79	2.33
	2	4.43	2.89
NOx			
	1	41.45	45.92
	2	242.11	196.39
NO_2			
	1	17.47	17.63
	2	26.80	26.44

TABLE III: Hourly average MAE in initial and final phase of sensor deployment. Phase 1 represents the initial 20 weeks and phase 2 represents the last 19 weeks. CM1 is the MAE using only pattern recognition techniques and CM2 is the MAE for proposed calibration model.

establishes a stronger case for the utility of time series analysis and simpler learning techniques in low-cost pollution sensing applications. The simpler learning techniques make minimal assumptions about the dataset and hence are unaffected by shift in data statistics. Another important point to note is that the results for MVLR have improved on using time series analysis, but the results for SVR remain unchanged. The reason for this zero improvement in SVR is the reliance of SVR algorithm on the learned support vectors. As the data statistics shift, the prediction accuracy of SVR gets worse. The errors for PLS have degraded slightly, but they are comparable to those obtained without using time series analysis. The following points regarding MVLR results should be noted. The R^2 and RMSE have improved in case of all pollutants. This shows that the proposed model is effective in capturing data variability. In table 1, R^2 was negative for many cases, while it is positive for almost all cases in table II. The RMSE is lowered in almost all cases in table II when compared with table I.

The improvement in MAE may seem small when comparing table I and II. This is not entirely correct and can be understood by closer examination of results. Table III and Figure 4 analyze the improvement in MAE from the temporal viewpoint. In figure 3, the errors are lower in the beginning but rise in the

This article has been accepted for publication in a future issue of this journal, but has not been fully edited. Content may change prior to final publication. Citation information: DOI 10.1109/TIM.2020.2976224, IEEE Transactions on Instrumentation and Measurement

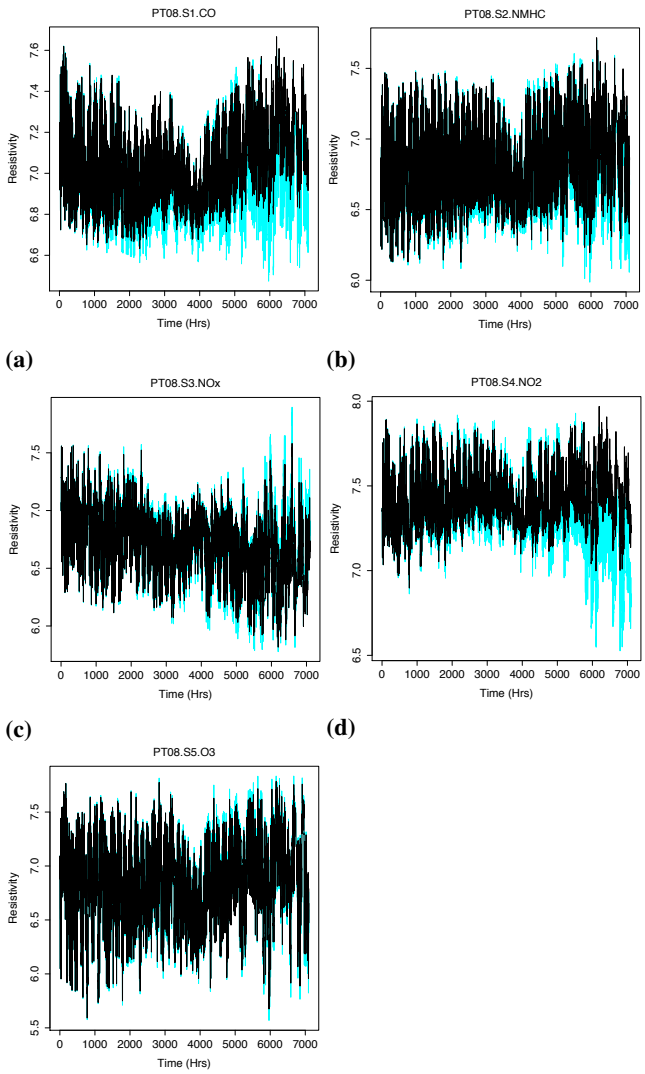

Fig. 3: Log transformed time series of sensor responses for the five sensors used in sensor array. The blue times series corresponds to the original sensor responses and the black sensor responses corresponds to the filtered sensor response. (a) PT08.S1.CO (b) PT08.S2.NMHC (c) PT08.S3.NOx (d) PT08.S4.NO2 (e) PT08.S5.O3. The notations for sensors corresponds to the ones used in UCI dataset [20]

later part. This increase is due to the sensor drift. The errors for the proposed scheme remain lower for the initial phase. This shows that the predicted time series is well-behaved. The errors in case of the proposed method are always lower for the latter part of time series as well. There are some peaks due to outliers, but in general, the proposed scheme has achieved its task of removing drift in sensor responses. Table III shows the improvement in hourly average mean absolute errors on a weekly basis. The proposed model has led to small increase in MAE for first 20 weeks of sensor deployment but it has been able to drastically reduce the errors for last 19 weeks of sensor deployment. The latter part of the sensor lifetime is the duration when sensors become unreliable due to the presence

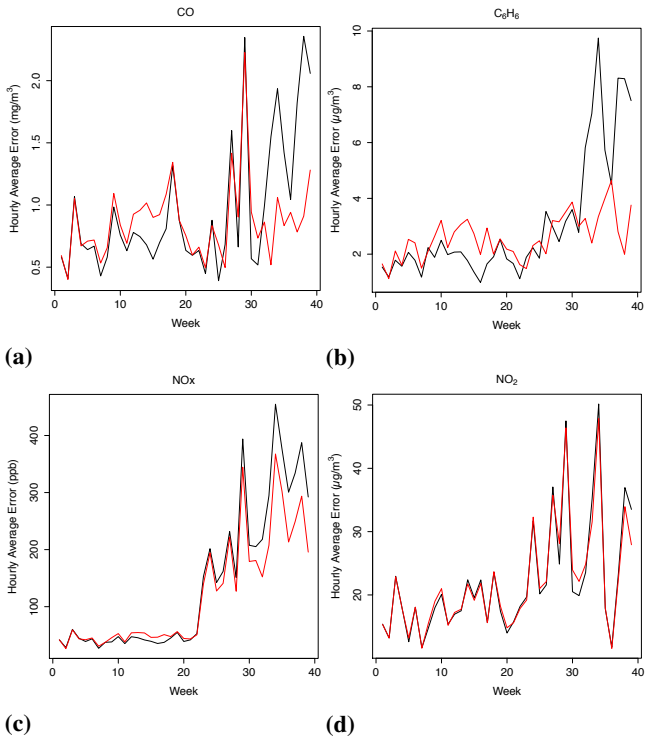

Fig. 4: Comparison of hourly average MAE on weekly basis between Prediction model using only MVLR (black) and Prediction model using Kalman filter bank followed by MVLR (red) for all pollutants (a) CO (b) C_6H_6 (c) NOx (d) NO_2. The value of $\alpha = 0.002$ was used for this result.

of large drift caused by sensor aging/poisoning. Except for NO_2, the proposed scheme improves the prediction accuracy for all pollutants.

It is to be noted that drift in chemical sensors is not present during the initial phase of the lifetime. This can be seen in the results of figure 3 and table III. It is only after a period of time that the sensor values start to drift due to deposition of contaminants on sensor film. There is an inherent advantage that simpler machine learning techniques have as compared to complex learning routines. The reliance of the simpler techniques on calibration data is much less than that of complex learning models since parameters of complex models are closely tuned to the calibration data. A Shift in data statistics is typical in air pollution sensing application and leads to performance degradation of complex models. The application of the Kalman filter is to bring the data statistics of the sensor response closer to that learned during the calibration. Any baseline removal technique can only reduce the effects of baseline drift and cannot completely remove it. Since the simpler techniques relied less on initial statistics the response to these improvements brought by filtering are more positive. The complex learning techniques require the statistics to be exactly similar to that of training data which no baseline removal technique can ensure. This is the inherent mechanism by which a combination of Kalman filtering and simple learners gives better results than any other methods and this can be seen in results of table II. The fact that the

This article has been accepted for publication in a future issue of this journal, but has not been fully edited. Content may change prior to final publication. Citation information: DOI 10.1109/TIM.2020.2976224, IEEE Transactions on Instrumentation and Measurement

	Interval	Training MAE	Test MAE	R^2	RMSE
CO					
	1	0.41	0.90	0.27	1.24
	2	0.44	0.85	0.43	1.11
C_6H_6					
	1	1.32	2.99	0.71	4.01
	2	1.44	2.36	0.81	3.29
NOx					
	1	26.59	133.73	-0.09	212.77
	2	30.12	122.81	0.09	198.17
NO_2					
	1	11.31	22.19	0.43	30.22
	2	12.38	22.69	0.46	29.84

TABLE IV: Comparison between training set lengths 300 hrs (Interval 1) and 700 hrs (Interval 2)

	Method	Training MAE	Test MAE	R^2	RMSE
CO					
	D1	0.39	0.91	0.21	1.29
	D2	0.54	1.06	0.05	1.43
	D3	0.42	1.22	-0.007	1.47
C_6H_6					
	D1	1.48	3.36	0.59	4.81
	D2	2.29	3.67	0.57	4.98
	D3	1.76	4.77	0.45	5.61
NOx					
	D1	26.21	137.19	-0.132	217.36
	D2	32.08	142.62	-0.17	222.47
	D3	28.27	138.18	-0.038	208.99
NO_2					
	D1	11.03	22.09	0.43	30.38
	D2	12.92	24.32	0.37	32.25
	D3	11.50	35.85	-0.26	45.44

TABLE V: Prediction accuracy results for other drift correction methods; D1: Baseline Removal using FFT, D2: Discrete Wavelet Transform, D3: Orthogonal Signal Correction

application of proposed adaptive Kalman filtering approach has improved the accuracy of simpler learning models is one of the major contributions of this study. This allows one to use simpler learning models with high R^2 values, thus assuring that the prediction error is independent of the shift in data statistics.

Table IV presents the results for training set lengths of 300 hrs and 700 hrs. These results have been presented for the case of Kalman filtering followed by linear regression. The value of α was taken to be 0.002. The comparison between time intervals 300 hrs and 500 hrs clearly show that a larger training set length leads to lower MAE and RMSE, and higher R^2 values. The comparison between time intervals 500 hrs and 700 hrs is slightly different. For the case of NO_x and NO_2, 500 hrs length seems to be more suitable. For the case of CO and C_6H_6, time interval of 700 hrs gives a slight improvement. This clearly indicates that an improvement in accuracy of prediction models with increase in training set lengths is speculative and is based on the sensor technology and the measurend in e-nose applications. For any factory calibration, optimal training lengths should be decided based on the experimental analysis as suggested in this study. The length of training set as 500 hrs seems to be appropriate for the use case in this study.

C. Comparison

This subsection presents the comparison of the proposed method with other relevant state of the art methods. The system model in each case is similar to the one shown in figure 1. The sensor responses are passed through a drift correction method and then the corrected responses are used as independent variables in a multivariate regression technique. In the proposed method, the combination of Kalman filtering and linear regression gives the best prediction accuracy. Therefore, it would be appropriate to compare other state of the art methods in the similar system model of drift correction followed by linear regression. As observed in section 2, very few drift correction methods in e-nose sensing literature are suitable for the open sampling use case studied in this paper. Some methods require time samples before and after the intake of gas in sensing chamber, some require a calibrant gas and some are only suitable for classification scenarios and cannot be used in quantification applications. The method suitable for comparison in accordance with the use case of this study are the ones which first correct the original sensor responses and then use the corrected responses for measurend prediction. Three drift correction techniques have been implemented for comparison. Specifically, methods based on baseline removal using FFT [22], Discrete Wavelet Transform (DWT) [27] and Orthogonal Signal Correction(OSC) [29] have been used. The results have been presented in table V. Figure 5 shows the original sensor response and drift corrected waveforms for the three methods. The baseline removal method is implemented using 'baseline.removal' function in package 'baseline' in R. The results show that the prediction accuracy of this method is less than the proposed method. It needs to be noted that the prediction accuracy is best among the other state of the art methods but there is caveat associated with this result. The baseline removal method is based on identifying baseline of a signal and removing it. The baseline also includes the information about the baseline of measurend values. Thus baseline removal also leads to loss of information about baseline of measurend values. The difference in baseline values of original and corrected waveforms is visible in figure 5(a)-(e). For this particular dataset, range of measurend values for calibration and test set was similar due to which removal of baseline did not effected the prediction accuracy. The method has performed well only beacuse it has been able to capture the original variance in the signal and has increased the dynamic range of waveform as observed in figure 5(a)-(e). The DWT method was implemented using 'waveShrink' function in wmtsa [46][47] package in R. Eighth order Daubechie (db8) was selected as the analyzing wavelet. It can be seen in table V that the prediction accuracy of the wavelet method is lower than that of the proposed method. The reason for this can be understood from figure 5(f)-(j). The original and corrected waveforms are almost identical and the algorithm has been unable to remove drifts in sensors. The major drawback of frequency transform based methods is that it is based on the assumption that drift occupies specific frequency bands which can never be the case for sensitivity and baseline drifts. Both DWT and baseline removal methods have an additional

This article has been accepted for publication in a future issue of this journal, but has not been fully edited. Content may change prior to final publication. Citation information: DOI 10.1109/TIM.2020.2976224, IEEE Transactions on Instrumentation and Measurement

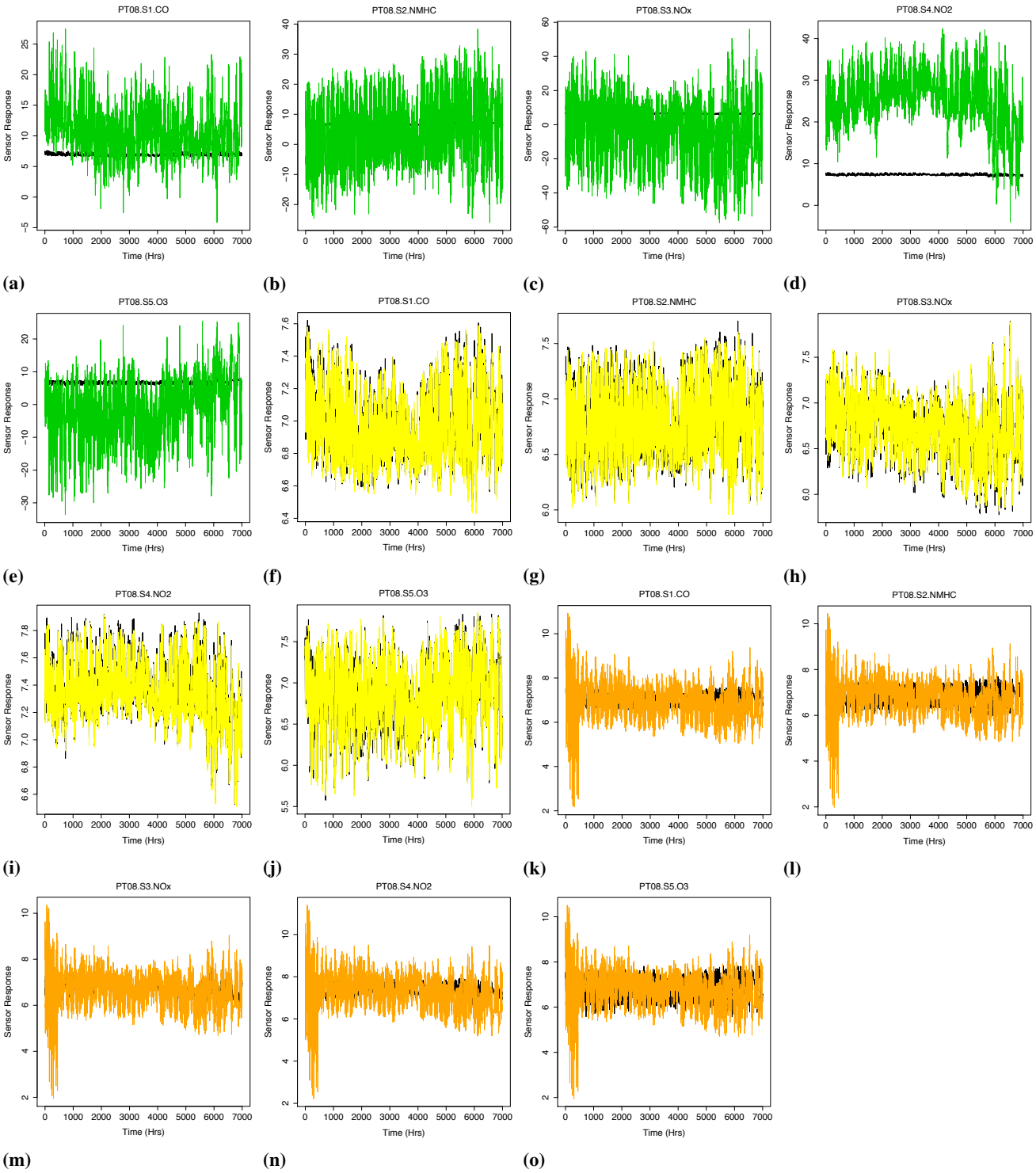

Fig. 5: Log transformed time series of sensor responses for the five sensors used in sensor array. The black times series corresponds to the original sensor responses. (a)-(e) Drift corrected waveform (green) using baseline removal method (D1), (f)-(j) Drift corrected waveform (yellow) using DWT method (D2), (k)-(o) Drift corrected waveform (orange) using OSC method (D3).

disadvantage. The frequency response can be evaluated only for an interval of data. Thus these algorithms cannot be used for applications requiring online drift corrections. The OSC method was implemented using Fearn's algorithm [30]. The results in this case are worse than the wavelet method. As explained in section II, the method relies completely on calibration data to identify factors to be subtracted from the data matrix. A shift in data statistics leads to degradation in noise removal capability of the OSC algorithm. As observed in figure 5(k)-(o), the algorithm increases the dynamic range for

initial period by removing the orthogonal component but has been unable to keep the similar dynamic range throughout the sensor lifetime. The variation in dynamic range of training and test set is the reason for underperformance of the OSC algorithm. It is to be noted that the adaptive nature of the proposed technique is its unique characteristic. It allows the method to constantly track data statistics in an online fashion and adapt its observation variance. Thus the method is immune to any shift in data statistics and its drift correction ability remains same throughout the sensor lifetime.

V. Conclusion and Future Scope

A calibration model for low-cost chemical sensor array has been proposed. The basic idea of improving prediction errors is based on the removal of baseline drifts from sensor signals. The baseline removal method is based on the time series analysis and Kalman filtering method. The parameter α plays a crucial role in adjusting the amount of drift in sensor responses. Factory calibration of sensors can help in determining the correct value of α for particular sensor technology and the chemical to be measured. The state of the art calibration models do not provide resistance to the shift in data statistics. This requirement is essential for the success of low-cost sensor technology for air pollution measurement and other applications. The proposed model captures the initial data statistics in terms of an AR process and drifts in terms of adaptive observation noise. These two information sources are then assimilated to predict correct sensor response, which is essentially drift-free.

Time series analysis can play a crucial role in increasing the accuracy of low-cost sensors. Extensive experimental research is required for characterizing time series process and drift parameters for sensors. It has been seen in this study and some earlier works [20] that sensor performance starts to degrade after a specific time. The proposed model can be implemented more effectively using the knowledge of lifetime of sensors. For example, the Kalman filter can be operated only after the initial phase of the sensor lifetime is completed. A higher resolution calibration data can help in correctly characterizing the sensor response. The suggested approach can also be used in other time series based chemical sensing applications.

References

[1] S. Bicelli, A. Depari, G. Faglia, A. Flammini, A. Fort, M. Mugnaini, A. Ponzoni, V. Vignoli, and S. Rocchi, "Model and experimental characterization of the dynamic behavior of low-power carbon monoxide mox sensors operated with pulsed temperature profiles," *IEEE Transactions on Instrumentation and Measurement*, vol. 58, no. 5, pp. 1324–1332, 2009.

[2] W. Jiao, G. Hagler, R. Williams, R. Sharpe, R. Brown, D. Garver, R. Judge, M. Caudill, J. Rickard, M. Davis *et al.*, "Community air sensor network (cairsense) project: evaluation of low-cost sensor performance in a suburban environment in the southeastern united states," *Atmospheric Measurement Techniques*, vol. 9, no. 11, pp. 5281–5292, 2016.

[3] M. Rossi and D. Brunelli, "Autonomous gas detection and mapping with unmanned aerial vehicles," *IEEE Transactions on Instrumentation and measurement*, vol. 65, no. 4, pp. 765–775, 2015.

[4] F. Chraim, Y. B. Erol, and K. Pister, "Wireless gas leak detection and localization," *IEEE Transactions on Industrial Informatics*, vol. 12, no. 2, pp. 768–779, 2015.

[5] L. Liu, G. Han, Y. He, and J. Jiang, "Fault-tolerant event region detection on trajectory pattern extraction for industrial wireless sensor networks," *IEEE Transactions on Industrial Informatics*, 2019.

[6] L. Zhang, Y. Liu, and P. Deng, "Odor recognition in multiple e-nose systems with cross-domain discriminative subspace learning," *IEEE Transactions on Instrumentation and Measurement*, vol. 66, no. 7, pp. 1679–1692, 2017.

[7] A. L. Clements, W. G. Griswold, A. RS, J. E. Johnston, M. M. Herting, J. Thorson, A. Collier-Oxandale, and M. Hannigan, "Low-cost air quality monitoring tools: From research to practice (a workshop summary)," *Sensors*, vol. 17, no. 11, p. 2478, oct 2017.

[8] S. Vikram, A. Collier-Oxandale, M. H. Ostertag, M. Menarini, C. Chermak, S. Dasgupta, T. Rosing, M. Hannigan, and W. G. Griswold, "Evaluating and improving the reliability of gas-phase sensor system calibrations across new locations for ambient measurements and personal exposure monitoring," *Atmospheric Measurement Techniques*, vol. 12, no. 8, pp. 4211–4239, 2019.

[9] N. Castell, F. R. Dauge, P. Schneider, M. Vogt, U. Lerner, B. Fishbain, D. Broday, and A. Bartonova, "Can commercial low-cost sensor platforms contribute to air quality monitoring and exposure estimates?" *Environment International*, vol. 99, pp. 293–302, feb 2017.

[10] T. Matthews, M. Iqbal, and H. Gonzalez-Velez, "Non-linear machine learning with active sampling for mox drift compensation," in *2018 IEEE/ACM 5th International Conference on Big Data Computing Applications and Technologies (BDCAT)*. IEEE, 2018, pp. 61–70.

[11] E. S. Cross, L. R. Williams, D. K. Lewis, G. R. Magoon, T. B. Onasch, M. L. Kaminsky, D. R. Worsnop, and J. T. Jayne, "Use of electrochemical sensors for measurement of air pollution: correcting interference response and validating measurements," *Atmospheric Measurement Techniques*, vol. 10, no. 9, pp. 3575–3588, sep 2017.

[12] M. J. Wenzel, A. Mensah-Brown, F. Josse, and E. E. Yaz, "Online drift compensation for chemical sensors using estimation theory," *IEEE Sensors Journal*, vol. 11, no. 1, pp. 225–232, 2010.

[13] A. Fort, S. Rocchi, M. B. Serrano-Santos, R. Spinicci, and V. Vignoli, "Surface state model for conductance responses during thermal-modulation of sno _{2}-based thick film sensors: Part imodel derivation," *IEEE transactions on instrumentation and measurement*, vol. 55, no. 6, pp. 2102–2106, 2006.

[14] S. Marco and A. Gutierrez-Galvez, "Signal and data processing for machine olfaction and chemical sensing: A review," *IEEE Sensors Journal*, vol. 12, no. 11, pp. 3189–3214, 2012.

[15] W. Li, H. Leung, C. Kwan, and B. R. Linnell, "E-nose vapor identification based on dempster–shafer fusion of multiple classifiers," *IEEE Transactions on instrumentation and measurement*, vol. 57, no. 10, pp. 2273–2282, 2008.

[16] S. K. Jha, K. Hayashi, and R. Yadava, "Neural, fuzzy and neuro-fuzzy approach for concentration estimation of volatile organic compounds by surface acoustic wave sensor array," *Measurement*, vol. 55, pp. 186–195, 2014.

[17] Y.-Q. Jing, Q.-H. Meng, P.-F. Qi, M.-L. Cao, M. Zeng, and S.-G. Ma, "A bioinspired neural network for data processing in an electronic nose," *IEEE Transactions on Instrumentation and Measurement*, vol. 65, no. 10, pp. 2369–2380, 2016.

[18] E. Phaisangittisagul and H. T. Nagle, "Predicting odor mixture's responses on machine olfaction sensors," *Sensors and Actuators B: Chemical*, vol. 155, no. 2, pp. 473–482, 2011.

[19] J. Burgués and S. Marco, "Multivariate estimation of the limit of detection by orthogonal partial least squares in temperature-modulated mox sensors," *Analytica chimica acta*, vol. 1019, pp. 49–64, 2018.

[20] S. De Vito, E. Massera, M. Piga, L. Martinotto, and G. Di Francia, "On field calibration of an electronic nose for benzene estimation in an urban pollution monitoring scenario," *Sensors and Actuators B: Chemical*, vol. 129, no. 2, pp. 750–757, 2008.

[21] R. Gutierrez-Osuna, "Signal processing methods for drift compensation," in *2nd NOSE II Workshop Linköping*, 2003, pp. 18–21.

[22] A. K. Atakan, W. Blass, and D. Jennings, "Elimination of baseline variations from a recorded spectrum by ultra-low frequency filtering," *Applied Spectroscopy*, vol. 34, no. 3, pp. 369–372, 1980.

[23] T. Nakamoto and H. Ishida, "Chemical sensing in spatial/temporal domains," *Chemical reviews*, vol. 108, no. 2, pp. 680–704, 2008.

[24] M. Nakamura, I. Sugimoto, H. Kuwano, and R. Lemos, "Chemical sensing by analysing dynamics of plasma polymer film-coated sensors," *Sensors and Actuators B: Chemical*, vol. 20, no. 2-3, pp. 231–237, 1994.

[25] S. Vembu, A. Vergara, M. K. Muezzinoglu, and R. Huerta, "On time series features and kernels for machine olfaction," *Sensors and Actuators B: Chemical*, vol. 174, pp. 535–546, 2012.

[26] K. Sothivelr, F. Bender, F. Josse, A. J. Ricco, E. E. Yaz, R. E. Mohler, and R. Kolhatkar, "Detection and quantification of aromatic hydrocarbon compounds in water using sh-saw sensors and estimation-theory-based signal processing," *ACS Sensors*, vol. 1, no. 1, pp. 63–72, 2015.

[27] M. Zuppa, C. Distante, K. C. Persaud, and P. Siciliano, "Recovery of drifting sensor responses by means of dwt analysis," *Sensors and Actuators B: Chemical*, vol. 120, no. 2, pp. 411–416, 2007.

[28] N. Nimsuk and T. Nakamoto, "Study on the odor classification in dynamical concentration robust against humidity and temperature changes," *Sensors and Actuators B: Chemical*, vol. 134, no. 1, pp. 252–257, 2008.

[29] S. Wold, H. Antti, F. Lindgren, and J. Öhman, "Orthogonal signal correction of near-infrared spectra," *Chemometrics and Intelligent laboratory systems*, vol. 44, no. 1-2, pp. 175–185, 1998.

[30] T. Fearn, "On orthogonal signal correction," *Chemometrics and intelligent laboratory systems*, vol. 50, no. 1, pp. 47–52, 2000.

[31] A. Perera, N. Papamichail, N. Bârsan, U. Weimar, and S. Marco, "On-line novelty detection by recursive dynamic principal component analysis and gas sensor arrays under drift conditions," *IEEE Sensors Journal*, vol. 6, no. 3, pp. 770–783, 2006.

[32] L. Zhang and D. Zhang, "Domain adaptation extreme learning machines for drift compensation in e-nose systems," *IEEE Transactions on instrumentation and measurement*, vol. 64, no. 7, pp. 1790–1801, 2014.

[33] K. Yan and D. Zhang, "Correcting instrumental variation and time-varying drift: a transfer learning approach with autoencoders," *IEEE Transactions on Instrumentation and Measurement*, vol. 65, no. 9, pp. 2012–2022, 2016.

[34] G. E. Box, G. M. Jenkins, G. C. Reinsel, and G. M. Ljung, *Time series analysis: forecasting and control*. John Wiley & Sons, 2015.

[35] B. D. Anderson and J. B. Moore, *Optimal filtering*. Courier Corporation, 2012.

[36] R. H. Shumway and D. S. Stoffer, *Time series analysis and its applications: with R examples*. Springer, 2017.

[37] S. D. Brown and S. C. Rutan, "Adaptive kalman filtering," *Journal of Research of the National Institute of Standards and Technology*, vol. 90, no. 6, pp. 403–407, 1986.

[38] A. Mohamed and K. Schwarz, "Adaptive kalman filtering for ins/gps," *Journal of geodesy*, vol. 73, no. 4, pp. 193–203, 1999.

[39] Q. Zhang, Y. Yang, Q. Xiang, Q. He, Z. Zhou, and Y. Yao, "Noise adaptive kalman filter for joint polarization tracking and channel equalization using cascaded covariance matching," *IEEE Photonics Journal*, vol. 10, no. 1, pp. 1–11, 2018.

[40] S. De Vito, E. Esposito, M. Salvato, O. Popoola, F. Formisano, R. Jones, and G. Di Francia, "Calibrating chemical multisensory devices for real world applications: An in-depth comparison of quantitative machine learning approaches," *Sensors and Actuators B: Chemical*, vol. 255, pp. 1191–1210, 2018.

[41] A. J. Smola and B. Schölkopf, "A tutorial on support vector regression," *Statistics and computing*, vol. 14, no. 3, pp. 199–222, 2004.

[42] E. E. Holmes, E. J. Ward, and K. Wills, "Marss: Multivariate autoregressive state-space models for analyzing time-series data." *R journal*, vol. 4, no. 1, 2012.

[43] G. Petris and R. An, "An r package for dynamic linear models," *Journal of Statistical Software*, vol. 36, no. 12, pp. 1–16, 2010.

[44] C.-C. Chang and C.-J. Lin, "Libsvm: A library for support vector machines," *ACM transactions on intelligent systems and technology (TIST)*, vol. 2, no. 3, p. 27, 2011.

[45] R. Wehrens and B.-H. Mevik, "The pls package: principal component and partial least squares regression in r," 2007.

[46] D. L. Donoho and I. M. Johnstone, "Adapting to unknown smoothness via wavelet shrinkage," *Journal of the american statistical association*, vol. 90, no. 432, pp. 1200–1224, 1995.

[47] D. B. Percival and A. T. Walden, *Wavelet methods for time series analysis*. Cambridge university press, 2000, vol. 4.

Abhishek Grover is pursuing Ph.D. in Indian Institute of Technology Delhi, New Delhi. He received his B.Tech in Electronics and Communication Engineering from Delhi Technological University, New Delhi in 2015. He completed his Masters of Science (Research) from Bharti School of Telecommunication Technology and Management, IIT Delhi in 2018. Broadly, his research area encompasses Embedded Systems and Signal Processing.

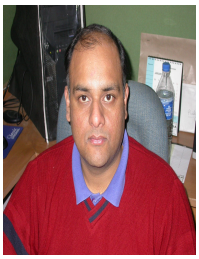

Brejesh Lall is Professor at Department of Electrical Engineering, Indian Institute of Technology Delhi, New Delhi. He received his B.Tech (Electronics and Communication Engineering) and Masters (Signal Processing) from Delhi College of Engineering, New Delhi. He did his Ph.D. in signal processing in 1999 from IIT Delhi.

Dr. lall joined Aricent in 1997. He joined IIT Delhi as Assistant Professor in 2005. He worked in the designation of Associate Professor from 2010 to 2018. He is actively working in the area of Image Processing, Signal Processing, and Communication. The areas include, object representation, tracking and classification, odometry, depth map generation, representation and rendering. He is also exploring vector sensor based underwater acoustic communications, and performance issues in molecular communications.